Chaotic Domain Structure in Rotating Convection

Yuhai Tu and M. C. Cross

Condensed Matter Physics, 114-36, Caltech, Pasadena, California 91125

(Received 7 August 1992)

Rotating convection near onset is studied using a three mode model but with the inclusion of spatial dependence. An apparently chaotic dynamics is found, consistent with experiment, without the necessity of adding *ad hoc* noise terms as in previous models. There is no phase transition approaching the point of linear instability of straight rolls from the disordered side, and the characteristic domain size and switching time remain finite here. This behavior is discussed in terms of the velocity of walls between the different domains.

PACS numbers: 47.25.−c, 05.45.+b, 47.20.Tg

Pattern formation in nonequilibrium systems has received a great deal of attention during the past two decades. One of the most studied systems is Rayleigh-Bénard thermal convection [1]. The study of rotating convection was directly motivated by the dynamics of planetary and stellar atmospheres and the circulation of ocean currents. In addition, due to the interplay between the thermal buoyancy and rotation-induced Coriolis force, the rotating thermal convection pattern has some very interesting characteristics which are absent in the nonrotating case. In particular, the system shows a novel nonlinear instability known as the Kuppers-Lorz (KL) instability [2] and is "nonpotential" arbitrarily close to threshold; i.e., there is no potential functional which monotonically decreases in the dynamics.

Kuppers and Lorz [2] showed that, when the dimensionless rotation rate Ω is greater than some critical value Ω_c, the originally stable pattern of straight rolls in an ideal laterally infinite system will lose its stability to another set of rolls at some angle θ_c relative to the original set. The new set will in turn lose its stability to another set at a further rotation θ_c, and so on, so that there is no stable steady-state pattern. Based on the fact that θ_c is very close to $2\pi/3$, Busse and Heikes (BH) [3] proposed a dynamical model consisting of three variables A_i $(i=1,2,3)$, which represent the amplitudes of three sets of rolls with relative orientation $2\pi/3$ to each other:

$$\tau_0 \partial A_i/\partial t = A_i \left(\epsilon - \sum_{j=1}^{3} g_{ij} |A_j|^2 \right) \quad (i=1,2,3)\,, \tag{1}$$

where $\epsilon=(R-R_c)/R_c$ is the reduced Rayleigh number and τ_0 sets the time scale. One can fix $g_{ii}=1$ for $i=1,2,3$; $g_{12}=g_{23}=g_{31}\equiv g_+$, $g_{21}=g_{32}=g_{13}\equiv g_-$ because of rotational symmetry; but $g_+\neq g_-$ due to lack of reflection symmetry.

The dependence of the coupling constants g_+, g_- on the rotation frequency was first calculated by Kuppers and Lorz [2,4]. The KL instability corresponds to $g_+ > 1$ and $g_- < 1$ (by convention, we will choose $g_+ \geq g_-$), and the critical rotation rate is determined by $g_- = 1$. In the range $g_- < 1$, Eq. (1) has no stable fixed point, and the dynamics of Eq. (1) is controlled by the heteroclinic orbit connecting the three unstable fixed points: $(\epsilon^{1/2},0,0)$, $(0,\epsilon^{1/2},0)$, $(0,0,\epsilon^{1/2})$, where (A_1,A_2,A_3) is the vector of amplitudes.

Starting with an arbitrary initial condition, the dynamics will drive the system towards the heteroclinic orbit, and the system will spend a longer and longer time in the vicinity of each fixed point before quickly switching to the vicinity of the next fixed point, and so on, so that the return time diverges at long time. (This phenomena has been previously shown in a different model by May and Leonard [5]). Busse and Heikes [3] suggested that this unphysical feature of the three mode model can be overcome by introducing noise. Because each of the fixed points is unstable, the orbit will approach the fixed point only up to a limit determined by the strength of the noise. In this way, a characteristic return time can be introduced.

The shortcoming of the BH model is the arbitrariness of the added noise. The physical nature of the noise is not clear: It could be due to thermal fluctuation, or experimental noise, or both, making it hard to quantify the theory. Also the spatially independent dynamical model does not give any description of the spatial pattern expected in a realistic physical system.

Recently, there has been renewed interest in rotating convection experiments [6,7], with a more careful investigation of the spatial structure revealed by high resolution shadowgraph imaging. As found by Bodenschatz *et al.* [8] in a large aspect ratio ($\Gamma=22$) experiment using dense CO_2, the complex time-dependent spatial pattern can be best described by the motion of domain walls separating patches of rolls with different orientations.

To study the spatial pattern of rotating convection, we modify the BH model by introducing the spatial dependence. This new model yields a return time without any *ad hoc* assumptions, and also predicts spatial patterns similar to ones seen experimentally. The spatial dependence is included by adding Newell-Whitehead-Segel [9,10] type terms in Eq. (1):

$$\tau_0 \frac{\partial A_i}{\partial t} = \xi_0^2 \left(\partial_{x_i} + \frac{1}{2iq_0} \partial_{y_i}^2 \right)^2 A_i + \left(\epsilon - \sum_{j=1}^{3} g_{ij} |A_j|^2 \right) A_i\,, \tag{2}$$

where $x_i = \mathbf{r}\cdot\hat{\mathbf{n}}_i$, $y_i = (\mathbf{r}\times\hat{\mathbf{n}}_i)\cdot\hat{\mathbf{z}}$, and $\hat{\mathbf{n}}_i$ is the unit vector normal to the ith roll so that $\hat{\mathbf{n}}_1$, $\hat{\mathbf{n}}_2$, and $\hat{\mathbf{n}}_3$ are unit vectors with relative angle 120° to each other. Also q_0 is the length of the most unstable wave vector, and ξ_0 is an order unity constant that may be calculated for each physical system.

Making the transformations $t \to \tau_0 t/\epsilon$, $\mathbf{r} \to \xi_0 \mathbf{r}/\sqrt{\epsilon}$, and $A_i \to \sqrt{\epsilon} A_i$, neglecting the higher-order terms in ϵ, and taking A_i to be real variables, we have

$$\partial A_1/\partial t = \partial_{x_1}^2 A_1 + A_1(1 - A_1^2 - g_- A_2^2 - g_+ A_3^2), \quad (3)$$

$$\partial A_2/\partial t = \partial_{x_2}^2 A_2 + A_2(1 - A_2^2 - g_- A_3^2 - g_+ A_1^2), \quad (4)$$

$$\partial A_3/\partial t = \partial_{x_3}^2 A_3 + A_3(1 - A_3^2 - g_- A_1^2 - g_+ A_2^2). \quad (5)$$

An important property of the above model is that the above equations are nonpotential due to lack of reflection symmetry, i.e., $g_- \neq g_+$.

We have studied the above equations numerically in two dimensions. For numerical convenience we add to the right-hand side of Eqs. (3)–(5) a term $\delta\partial_{y_i}^2 A_i$ with small $\delta \ll 1$. In the following we set $\delta = 0.1$ (it can be shown that $\delta \to 0$ is a smooth limit). We also fix the value of $g_+ = 2$ and let g_- be the only varying parameter in our model. We use a pseudospectral method to integrate the equations on a square mesh with the system size $L = 64$, 96, and 128 and periodic boundary conditions. (A mesh size of $\Delta x = 1$ and time step $\Delta t = 0.01$ provide sufficient resolution.)

We start our numerical calculation with an initial condition of small random fluctuations. To monitor the growth of the pattern, we can define a quantity $Q(t) = L^{-2}\int (A_1^2 + A_2^2 + A_3^2) d^2 r$. We find that after an initial stage of exponential growth, Q increases slowly by merging of small patches which have the same orientation. This process is eventually balanced by the motion of domain walls between domains which have different orientation order. Finally the system approaches a statistical steady state where the average number of domains and the average size of each domain do not change with time. A typical pattern at this stage is shown in Fig. 1(a) for $g_- = 0.5$.

We have also depicted the time dependence of the three amplitudes at a specific point in space in Fig. 1(b) for the same run. As in the original BH model, the pattern at a specific point is successively dominated by the three states. Also there is a characteristic switching time scale T given by the center of the peak in the power spectrum. Its dependence on g_- will be discussed later.

We can define a quantitative measurement of the spatial structure of the statistical steady state of our model. A useful quantity is the equal time correlation function:

$$C_1(\mathbf{r}) = \frac{\langle A_1(\mathbf{r}+\mathbf{r}_0, t_0) A_1(\mathbf{r}_0, t_0)\rangle - \langle A_1(\mathbf{r}_0, t_0)\rangle^2}{\langle A_1^2(\mathbf{r}_0, t_0)\rangle - \langle A_1(\mathbf{r}_0, t_0)\rangle^2}, \quad (6)$$

where $\langle\ \rangle$ represents an average over $\mathbf{r}_0$ and t_0. The profile of $C_1(\mathbf{r})$ along the (1,1) direction is shown in Fig. 2(a). [$C_1(\mathbf{r})$ is anisotropic due to the anisotropy of the equation of motion, but only weakly.] We define a correlation length or domain size as

$$\xi = \frac{\int C_1^2(\mathbf{r}) d\mathbf{r}}{[8\int C_1^4(\mathbf{r}) d\mathbf{r}]^{1/2}}. \quad (7)$$

Note that this definition emphasizes the region over which the correlation is large rather than the asymptotic large distance region.

As expected, the correlation length ξ increases as we increase g_-, which physically corresponds to decreasing the rotation frequency Ω. But surprisingly, as g_- approaches the KL instability point $g_- = 1$, ξ still remains finite. We have carried out our calculation even into the region where an ideal roll state is not subject to the KL instability, i.e., for $g_- > 1$. If we start with random initial conditions, the dynamics is qualitatively the same as the case with $g_- < 1$. The inverse correlation length versus g_- is plotted in Fig. 2(b) together with the inverse time scale. Both length scale and time scale remain finite

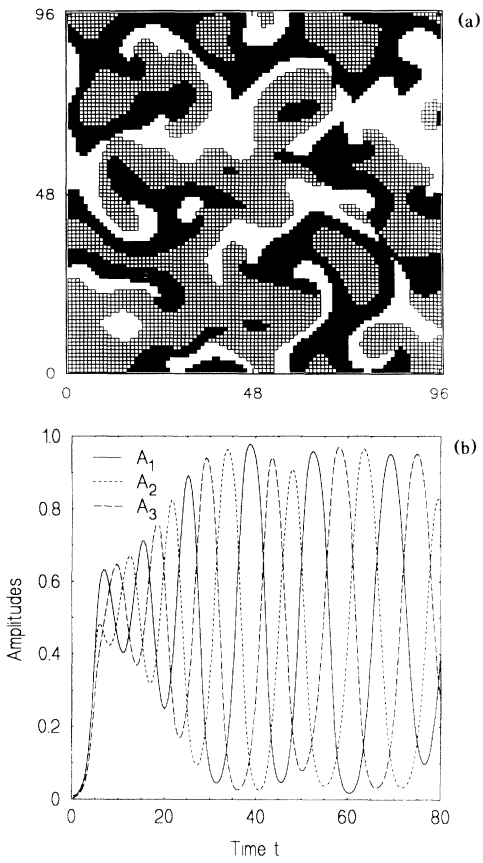

FIG. 1. (a) A snapshot of the spatial pattern in the statistical steady state given by simulating Eqs. (3)–(5) with $g_+ = 2.0$ and $g_- = 0.5$. The dark, gray, and light regions represent the areas occupied by A_1, A_2, and A_3, respectively. (The region of occupancy is determined by the maximum of the three amplitudes at each point.) (b) Time dependence of the amplitudes at the center of the cell.

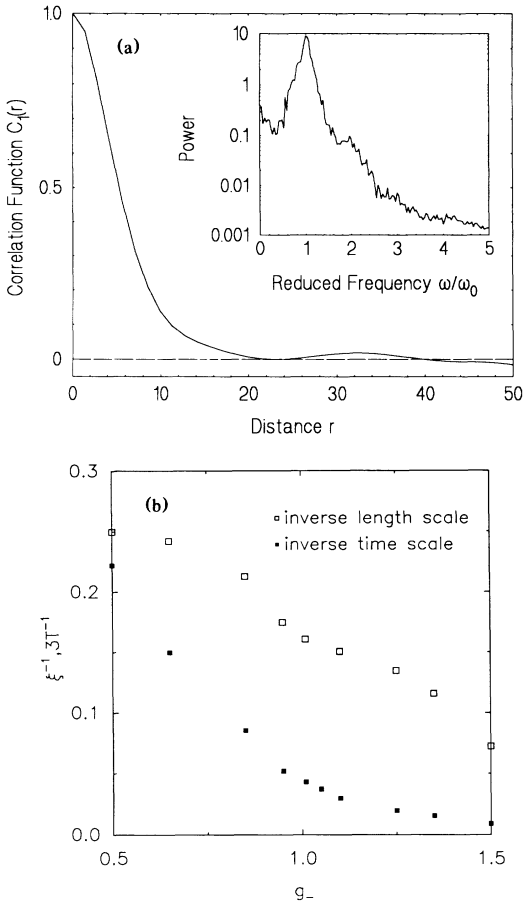

FIG. 2. (a) The normalized correlation function along the (1,1) direction for the same parameters as in Fig. 1. Inset: The power spectrum of amplitude time series as shown in Fig. 1(b). (b) The inverse correlation length and the inverse switching time scale vs g_- for $g_+ = 2.0$.

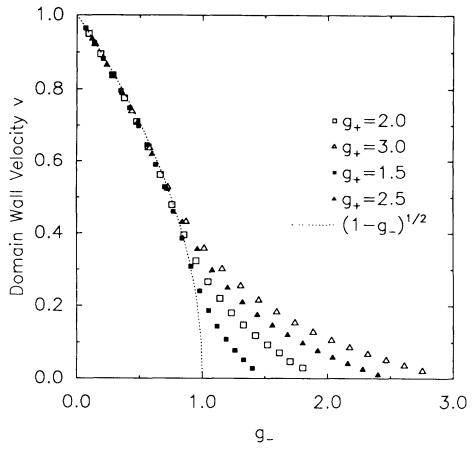

FIG. 3. The domain wall velocity v vs g_- for various values of g_+ given by the numerical simulation of the one-dimensional Eqs. (8) and (9). The dotted line represents the velocity determined by the linear selection criteria.

at $g_- = 1$, with no indication of critical behavior here.

This observation is quite intriguing. As we know, for potential systems, adding a diffusion term will not change the structure of a spatially uniform bifurcation, simply because the term $(\nabla\phi)^2$ (ϕ is the order parameter) in the potential, which is responsible for the diffusion term in the dynamical equation, favors a spatially uniform pattern. In the present case, the addition of the diffusion term creates a new spatially dependent and apparently chaotic attractor for the system. This attractor appears to be the only stable structure for $g_- < 1$, and it persists for $g_- > 1$.

The existence of this complex state for $g_- > 1$ can be understood as follows. In the original BH model, the basins of attraction for different fixed points are quite tangled, unlike the basins in a potential system, which have a very simple structure. In this situation, a small fluctuation, such as caused by spatial coupling to other domains, can easily cause a point in phase space to jump from the basin of one fixed point to that of another fixed point, and the system never settles down to any one of the fixed points.

The numerical simulations suggest that the dynamics of this system can be described in terms of the motion of domain walls separating regions occupied by different sets of rolls [11]. Therefore a useful way to analyze the problem is to study the motion of a domain wall separating, for example, A_1 and A_2. Suppose the domain wall is at some angle θ_0 relative to the first set of rolls. If we neglect the motion along the domain wall, the problem becomes essentially one dimensional:

$$\partial_t A_1 = \cos^2\theta_0 \partial_y^2 A_1 + A_1(1 - A_1^2 - g_- A_2^2), \quad (8)$$

$$\partial_t A_2 = \cos^2(2\pi/3 - \theta_0)\partial_y^2 A_2 + A_2(1 - A_2^2 - g_+ A_1^2), \quad (9)$$

where y is the coordinate perpendicular to the domain wall, with the asymptotic behavior $A_1 \to 1$, $A_2 \to 0$ as $y \to -\infty$ and $A_1 \to 0$, $A_2 \to 1$ as $y \to \infty$.

We look for a steady moving solution with the form $A_1(y,t) = A_1(z)$, $A_2(y,t) = A_2(z)$, where $z = y - vt$. For $g_- > 1$, the domain wall velocity v between two stable states is uniquely determined and goes to zero as $g_- \to g_+$. For $g_- < 1$, where the domain wall is propagating into an unstable state, there is a continuous spectrum of possible steady moving solutions. There has been much work on the question of the dynamical selection of a particular member of this family [12]. A linear velocity selection criterion predicts a velocity $v^* = 2(1-g_-)^{1/2} \times \cos\theta_0$. Notice that $v^* \to 0$ as $g_- \to 1$, which means there would be a transition at $g_- = 1$. As shown in Fig. 3 for $\theta_0 = \pi/3$, the velocity calculated numerically from a simulation of Eqs. (8) and (9) does follow the relation $v = (1-g_-)^{1/2}$ for $g_- < g_-^*(g_+, \theta_0) < 1$, but for $g_- > g_-^*(g_+, \theta_0)$, it deviates significantly and is finite at $g_- = 1$. The velocity selection in the interval $g_-^*(g_+, \theta_0) < g_- < 1$ is presumably controlled by the nonlinear

selection criterion [13]. This predicts a velocity which connects smoothly with the unique velocity for $g_- > 1$, as is seen in Fig. 3. Note that there is no discontinuous change in the domain wall velocity predicted from this picture at $g_- = 1$, which is consistent with the absence of a transition in the two-dimensional numerics. We point out, however, that the selection criteria for $g_- < 1$ are usually derived in terms of the asymptotic state developing from a localized initial condition in an otherwise uniform system. The relevance of these criteria to the present case is by no means clear. It will therefore be interesting to study the spectrum of 2D domain wall velocities for $g_- < 1$ to see if a unique velocity is selected (for a given domain wall angle), or if instead a distribution is found, changing to a unique one for $g_- > 1$.

In the limit $g_- = g_+$, the system becomes potential. In this case, the final state of the system is expected to break the symmetry between A_1, A_2, and A_3 and to consist of only one set of rolls. The question now is for given value of g_+, where does the transition occur on the g_- axis between 1 and g_+? Our numerical results seem to suggest the transition takes place at $g_- = g_-^c < g_+$. Further investigation is needed to define this transition.

To sum up our paper, we have studied the spatiotemporal behavior of rotating convection patterns near onset using a simple model of three spatially dependent amplitude equations. In agreement with experiment, the spatial pattern appears to be dominated by domain wall motion. We find that the time-dependent spatial pattern can be characterized by domains with a typical size (returning to unscaled units) $\xi_0 \xi(g_-, g_+)/\sqrt{\epsilon}$. The introduction of the spatial dependence also eliminates the necessity of adding noise as in the BH model. Instead, our model has a natural characteristic time $\tau_0 T_0(g_-, g_+)/\epsilon$. It will be interesting to measure the characteristic domain size and switching time experimentally and compare with the results of this model. Furthermore, we have found that, with spatial coupling, there is no transition approaching the KL instability point from the disordered state, i.e., the time-dependent disordered pattern persists for $\Omega < \Omega_c$. Experimentally, time-dependent patterns have indeed been observed at rotation rates lower than the KL threshold [7].

Clearly, to understand the experiments in more detail, it is desirable to study a model that includes the full range of possible roll orientations as well as boundaries. We have constructed a modified Swift-Hohenberg [14] model to accomplish this, and preliminary results compare well with experiment. These results, together with a more detailed account of the present results, will be presented in a future publication.

This work was supported by the National Science Foundation through Grant No. DMR-9013984. Yuhai Tu would like to acknowledge support by Caltech through a Division Postdoctoral Fellowship.

[1] For a recent review on this subject, see M. Cross and P. Hohenberg, "Pattern Formation Outside of Equilibrium," (to be published).
[2] G. Kuppers and D. Lorz, J. Fluid Mech. **35**, 609 (1969).
[3] F. H. Busse and F. H. Heikes, Science **208**, 173 (1980).
[4] G. Kuppers, Phys. Lett. **32A**, 7 (1970).
[5] R. M. May and W. J. Leonard, SIAM J. Appl. Math. **29**, 243 (1975).
[6] F. Zhong, R. E. Ecke, and V. Steinberg, Phys. Rev. Lett. **67**, 2473 (1991).
[7] F. Zhong, R. E. Ecke, and V. Steinberg, Physica (Amsterdam) **51D**, 596 (1991).
[8] E. Bodenschatz, D. S. Cannell, R. Eckes, Y. Hu, K. Lerman, and G. Ahlers (to be published).
[9] A. C. Newell and J. A. Whitehead, J. Fluid Mech. **38**, 279 (1969).
[10] L. A. Segel, J. Fluid Mech. **38**, 279 (1969).
[11] The amplitudes shown in Fig. 1(b) are not obviously characteristic of the motion of uniform domains separated by sharp walls. This is due to the fact that at $g_- = 0.5$ the size of the domains is comparable to the width of the walls. For larger g_- the domain walls are better defined, and for smaller g_-, corresponding to a larger rotation frequency, the domain structure is destroyed and the pattern becomes cellular.
[12] E. Ben-Jacob, H. R. Brand, G. Dee, L. Kramer, and J. S. Langer, Physica (Amsterdam) **14D**, 348 (1985); W. Van Saarloos, Phys. Rev. A **37**, 211 (1988).
[13] W. Van Saarloos, Phys. Rev. A **39**, 6369 (1989); W. Van Saarloos and P. C. Hohenberg, Physica (Amsterdam) **56D**, 303 (1992).
[14] J. B. Swift and P. C. Hohenberg, Phys. Rev. A **15**, 319 (1977).